



Hierarchical particle swarm optimizer for minimizing the non-convex potential energy of molecular structure



Ngaam J. Cheung, Hong-Bin Shen*

Institute of Image Processing and Pattern Recognition, Shanghai Jiao Tong University, Key Laboratory of System Control and Information Processing, Ministry of Education of China, 800 Dongchuan Road, Shanghai 200240, China

ARTICLE INFO

Article history:

Accepted 8 October 2014

Available online 18 October 2014

Keywords:

Particle swarm optimization

Molecular conformation

Heterogeneous search

Hierarchical group

Swarm migration

ABSTRACT

The stable conformation of a molecule is greatly important to uncover the secret of its properties and functions. Generally, the conformation of a molecule will be the most stable when it is of the minimum potential energy. Accordingly, the determination of the conformation can be solved in the optimization framework. It is, however, not an easy task to achieve the only conformation with the lowest energy among all the potential ones because of the high complexity of the energy landscape and the exponential computation increasing with molecular size. In this paper, we develop a hierarchical and heterogeneous particle swarm optimizer (HHPSO) to deal with the problem in the minimization of the potential energy. The proposed method is evaluated over a scalable simplified molecular potential energy function with up to 200 degrees of freedom and a realistic energy function of pseudo-ethane molecule. The experimental results are compared with other six PSO variants and four genetic algorithms. The results show HHPSO is significantly better than the compared PSOs with p -value less than 0.01277 over molecular potential energy function.

© 2014 Elsevier Inc. All rights reserved.

1. Introduction

It is greatly important to figure out the three-dimensional (3D) structure of a molecule, because the structure is essential to uncover the secret of its functions and properties in living organism. This motivates the prediction of the most stable conformation only depending on the energetics of the interactions between the atoms composing the molecule [1]. These energetics can be formulated as a mathematical description with numerous parameters of a molecule, and then the determination of these parameters becomes a continuous global minimization problem [2–4]. For instances, Maranas and Floudas propose an optimization algorithm and derive convex lower bounding function for searching the minimum energy of small molecules based on partitioning strategy and lower and upper bounds to guarantee the conformation of a molecule with the minimum energy [1]. In Ref. [2], the authors develop a continuous variable neighborhood search (VNS) heuristic to minimize the potential energy function of a molecule.

Particle swarm optimization (PSO) is a swarm-based intelligence algorithm developed by Kennedy and Eberhart in 1995 [5]. PSO simulates the behavior of a bird flock searching for food.

Each member modifies its flight direction by learning from its own experience and the experience of other members. Kennedy et al. successfully interpret these features into an optimization algorithm. Since PSO was proposed, numerous variants have been developed to improve its performance. The researchers focus on different terms to enhance the search ability of PSO involving keeping balance between exploration and exploitation by inertia weight [6–9], designing topological structures [10–12], using multi-swarm strategies [13,14], and employing heterogeneous update laws [13–15]. It is an efficient method to combine the multi-swarm strategies with heterogeneous update laws, for example, in Ref. [13], a taxonomy of heterogeneous PSO algorithm was proposed according to the strategies employed for exploring the optimization problems. They also classified the heterogeneous particles in accordance with the type of heterogeneity the swarms exhibit. Leonard et al. developed a dynamic heterogeneous particle swarm optimizer, which can dynamically manage the diversity of the swarm and track an optimal moving direction [15].

Many researchers have focused on hierarchical PSOs [8,16–18], for example, in [16] H-PSO was developed by designing a neighborhood structure in a dynamic hierarchy, and each particle moves up or down the hierarchy depending on its quality. The variant of H-PSO is to assign different behavior to the individual particles with respect to their level in the hierarchy. A memetic computing model was proposed based on hierarchical particle swarm

* Corresponding author. Tel.: +86 21 34205320; fax: +86 21 34204022.
E-mail address: hbshen@sjtu.edu.cn (H.-B. Shen).

optimizer (HPSO) and latin hypercube sampling (LHS) method [17]. In Ref. [18], the authors developed particle swarm optimization based clustering, which combines the qualities of hierarchical and partitional clustering to cluster data in a hierarchical agglomerative manner. A hierarchical cluster-based multispecies PSO was proposed for fuzzy-system optimization, in which a swarm is clustered into multiple species at an upper hierarchical level, and each species is further clustered into multiple subspecies at a lower hierarchical level [19]. In Ref. [20], HPSO with dynamic local neighborhood was developed within each dynamic hierarchy and based on multi-swarms. Different from the existing multi-swarm PSOs and hierarchical PSOs, a hierarchical heterogeneous particle swarm optimizer, denoted as HHPSO, is proposed to provide a novel insight on finding the three-dimensional structure of a molecule. In HHPSO, three hierarchical groups are to accomplish different tasks based on associate heterogeneous update laws during the optimization process. These sub-swarms involve excellent groups (EG), affiliated particles (AG), and potential particles (PG). In each group, the particles execute heterogeneous search laws instead of trying to achieve a compromise between exploration and exploitation by only one swarm and homogeneous strategy. To highly coordinate with the PG, we develop a probability-based swarm migration to enhance the capability of the standard PSO.

The rest of the article is organized as follows: Section 2 presents the simplified potential energy function of a molecule and a pseudo-ethane molecule. In Section 3, the proposed HHPSO algorithm is described in detail. Section 4 presents parameter settings and analysis of HHPSO, and also experimental results and discussion over the problems of minimizing the potential energy of a scalable molecular function and a pseudo-ethane molecule. Conclusions are given in Section 5.

2. Problem formulation

The potential energy of a molecule consists of several energy items, which are derived from molecular mechanics based on the principles of Newtonian physics. These energy items are used to describe the molecular interactions and considered as a force field [2]. The optimization of a molecule is to find the most suitable parameters of the force field in highly agreeing with experimental data.

The molecular model contains a chain of N atoms centered at x_1, x_2, \dots, x_N ($x_i \in \mathbb{R}^3$). Let $b_{i,i+1}$ be the Euclidean distance between each pair of consecutive atoms x_i and x_{i+1} , $\theta_{i,i+1}$ be the bond angle corresponding to the third atom x_{i+2} with respect to the line containing the previous two, and $\phi_{i,i+3}$ be the torsion angle, between the normals through the planes determined by the atoms x_i, x_{i+1}, x_{i+2} and $x_{i+1}, x_{i+2}, x_{i+3}$. The force field corresponding to bond lengths, bond angles, torsion angles, and interactions between every pair of atoms separated by more than two covalent bonds along the chain is formulated as follows [2]:

$$E_{LAT} = \sum_{(i,j) \in S_1} \alpha_{ij}^1 (b_{ij} - b_{ij}^\circ)^2 + \sum_{(i,j) \in S_2} \alpha_{ij}^2 (\theta_{ij} - \theta_{ij}^\circ)^2 + \sum_{(i,j) \in S_3} \alpha_{ij}^3 [1 + \cos(3\omega_{ij} - \omega_{ij}^\circ)] + \sum_{(i,j) \in S_3} \left[\frac{(-1)^i}{r_{ij}} \right] \quad (1)$$

where α_{ij}^1 , α_{ij}^2 and α_{ij}^3 are the force constants of bond stretching, angle bending and torsion, respectively. b_{ij} , θ_{ij} and ω_{ij} are bond length, bond angle and phase angle, respectively. b_{ij}° , θ_{ij}° and ω_{ij}° are the desired bond length, bond angle and phase angle, respectively. $S_{k,k=1,2,3}$ denotes the set of pairs of atoms separated by k covalent bonds, and r_{ij} is the Euclidean distance between atoms x_i and x_j .

In most cases, it is assumed that all covalent bond lengths and covalent bond angles are fixed at b_{ij}° and θ_{ij}° , respectively, in the molecular structure prediction [21]. The most stable conformation of a molecule is the one with the minimum energy, and, accordingly, it is the task to find the global minimum of E_{LAT} rewritten in Eq. (2).

$$E_{LAT} = \sum_{(i,j) \in S_3} [1 + \cos(3\omega_{ij})] + \sum_{(i,j) \in S_3} \left[\frac{(-1)^i}{r_{ij}} \right] \quad (2)$$

To reduce the freedom, we express the energy function in Eq. (1) in torsion angles. Let x_i, x_j, x_k and x_t be any four consecutive atoms in a chain of a molecule, then the relationship between the Euclidean distance and the torsion angle can be formulated as follows,

$$r_{it}^2 = r_{ij}^2 + r_{jt}^2 - \left(\frac{r_{jt}^2 + r_{jk}^2 - r_{kt}^2}{r_{jk}} \right) r_{ij} \cos(\theta_{ik}) - \left(\frac{\sqrt{4r_{jt}^2 r_{jk}^2 - (r_{jt}^2 + r_{jk}^2 - r_{kt}^2)^2}}{r_{jk}} \right) r_{ij} \sin(\theta_{ik}) \cos(\omega_{it}) \quad (3)$$

As a general optimization problem, it is to find the global minimization of the total molecular potential energy function as shown in Eq. (1). Since it is difficult to directly deal with the molecular model in full-atom, we reduce the model to a chain only containing carbon atoms. It has been observed that the bond lengths subject to a Gaussian distribution with a small standard deviation in high resolution protein structural data [21]. In reduced model, it can be easy to fix the desired bond length and bond angle in $b_{ij}^\circ = 1.526\text{\AA}$, ($\forall(i,j) \in S_1$) and $\theta_{ij}^\circ = 1.91\text{ rad}$, ($\forall(i,j) \in S_2$), respectively. Considering that $\alpha_{ij}^1 = 1$, ($\forall(i,j) \in S_1$), $\alpha_{ij}^2 = 1$, ($\forall(i,j) \in S_2$), $\alpha_{ij}^3 = 1$, ($\forall(i,j) \in S_3$), and $\omega_{ij}^\circ = 0$, $\forall(i,j) \in S_3$, Eq. (3) can be calculated and rewritten as shown in Eq. (4).

$$r_{ij} = \sqrt{10.60099896 - 4.141720682 \cos(\omega_{ij})}, \quad \forall(i,j) \in S_3 \quad (4)$$

According to Eqs. (2) and (4), we can obtain the further simplified energy function based on the established result in [2,22] as follows,

$$E_{LAT} = \sum_{(i,j) \in S_3} \left(1 + \cos(3\omega_{ij}) + \frac{(-1)^i}{\sqrt{10.60099896 - 4.141720682 \cos(\omega_{ij})}} \right) \quad (5)$$

where $i = 1, 2, \dots, N-3$, $j = i+3$, and N is the number of atoms in a given system.

Although the molecular potential energy function is simplified, it still contains 2^{N-3} local minimizers and is highly complex to be dealt with [22]. If $\omega_{ij} \in [0, 5]$, ($\forall(i,j) \in S_3$), the existence of only one global minimizer is guaranteed, and the global solution is the alternate sequence of torsion angles given by $\varepsilon, \xi, \varepsilon, \xi, \varepsilon, \xi, \dots$, where $\varepsilon = 1.039195303$ and $\xi = 3.141592654$. The landscape of the energy function is illustrated in Fig. 1 with only two variables. Accordingly, the problem of fixing the value of ω_{ij} is converted to an optimization of searching the global minimum of E_{LAT} in the search space $\omega_{ij} \in [0, 5]$. It is still not an easy task to solve the problem in reduced potential energy function because of numerous local minimums, for example, a molecule with only 20 atoms, the number of the local minimums is up to $2^{20-3} = 131,072$.

2.1. Potential energy function of a pseudo-ethane molecule

The model of a pseudo-ethane molecule was developed by Maranas and Floudas [1]. In the ethane molecule, all three

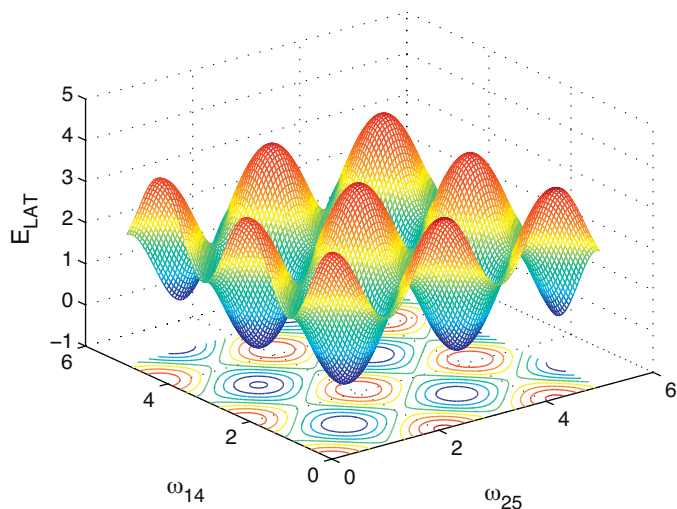


Fig. 1. Landscape of the simplified energy function with two variables.

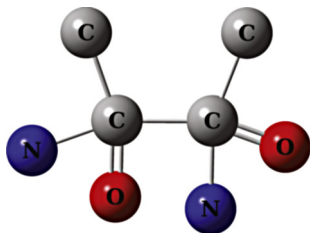


Fig. 2. A conceptual visualization of pseudo-ethane molecule.

hydrogen atoms of both carbon atoms are substituted by one carbon (C), one oxygen (O) and one nitrogen (N) atom as shown in Fig. 2.

As shown, it is an one dimensional problem of minimizing the potential energy for pseudo-ethane molecule. In Ref. [1], the potential energy of the pseudo-ethane molecule is defined by the Lennard–Jones potential, which is dominated by a single dihedral angle. The mathematical model is formulated as follows,

$$E_{PE} = \frac{588600}{[3b_0^2 - 4\cos(\theta_0)b_0^2 - 2(\sin^2(\theta_0)\cos(\phi - 2\pi/3) - \cos^2(\theta_0))b_0^2]^6} - \frac{1079.1}{[3b_0^2 - 4\cos(\theta_0)b_0^2 - 2(\sin^2(\theta_0)\cos(\phi - 2\pi/3) - \cos^2(\theta_0))b_0^2]^3} + \frac{600800}{[3b_0^2 - 4\cos(\theta_0)b_0^2 - 2(\sin^2(\theta_0)\cos(\phi) - \cos^2(\theta_0))b_0^2]^6} - \frac{1071.5}{[3b_0^2 - 4\cos(\theta_0)b_0^2 - 2(\sin^2(\theta_0)\cos(\phi) - \cos^2(\theta_0))b_0^2]^3} + \frac{481300}{[3b_0^2 - 4\cos(\theta_0)b_0^2 - 2(\sin^2(\theta_0)\cos(\phi + 2\pi/3) - \cos^2(\theta_0))b_0^2]^6} - \frac{1064.6}{[3b_0^2 - 4\cos(\theta_0)b_0^2 - 2(\sin^2(\theta_0)\cos(\phi + 2\pi/3) - \cos^2(\theta_0))b_0^2]^3} \quad (6)$$

where b_0 is covalent bond length ($b_0 = 1.54\text{\AA}$), θ_0 is covalent bond angle ($\theta_0 = 109.5^\circ$), ϕ is dihedral angle ($\phi \in [0, 2\pi]$).

To minimizing the molecular potential energy functions, many researchers have focused on the problem using various search techniques, such as genetic algorithm (GA) [23], simulated annealing (SA) [24], α BB algorithm [25], and particle swarm optimization

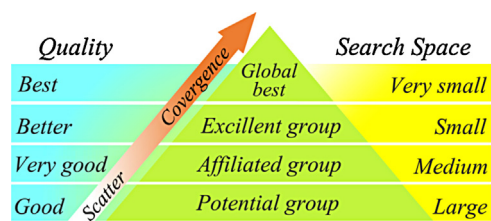


Fig. 3. Conceptual vision of the hierarchical groups in HHPSO.

(PSO) [3,4]. In this study, we develop a novel variant of PSO algorithm with hierarchical topology and heterogeneous search strategies to deal with the minimization of the non-convex potential energy in molecular structure. More details are presented in Section 3.

3. Hierarchical heterogeneous particle swarm optimizer

Particle swarm optimization (PSO), developed by Kennedy and Eberhart [5], consists of a collection of particles, which stand for the potential solutions to an optimization problem, including engineering problems [26–29]. The i th particle \mathbf{x}_i searches a D -dimension space to obtain the solution. Each particle adjusts its direction according to a weighted sum involving its position and new velocity, and this new velocity \mathbf{v}_i is determined by its previous velocity, the known previous best position (\mathbf{p}_i) and the global best position (\mathbf{g}_{best}). The i th particle's position and velocity are updated according to Eqs. (7) and (8).

$$\mathbf{v}_i(k+1) \leftarrow \omega \cdot \mathbf{v}_i(k) + c_1 \cdot \mathbf{r}_1 \cdot (\mathbf{p}_i - \mathbf{x}_i(k)) + c_2 \cdot \mathbf{r}_2 \cdot (\mathbf{g}_{best} - \mathbf{x}_i(k)) \quad (7)$$

$$\mathbf{x}_i(k+1) \leftarrow \mathbf{x}_i(k) + \mathbf{v}_i(k+1) \quad (8)$$

where c_1 and c_2 are both positive constants, which are called cognitive and social parameters, respectively. $\mathbf{r}_1, \mathbf{r}_2$ are vectors consisting of D random number generated from a uniform random distribution function in the interval $[0, 1]$. ω stands for the inertia weight, which is used to balance global search increasing swarm diversity and local search reducing diversity in the swarm.

3.1. The proposed HHPSO algorithm

In developed HHPSO algorithm, we hierarchically classify the whole population into three groups, which execute heterogeneous search laws. Fig. 3 illustrates the hierarchical structure of HHPSO, in which the three groups involve potential group (PG), affiliated group (AG) and excellent group (EG) (from bottom to top). The process is sketchily illustrated in Fig. 3, and the quality of the best-so-far solution becomes better as the size of search space decreasing. All these trends can lead the whole population converge from 'scatter'.

In the design, we employ the Eulerian distance d to determine which group the particle belongs to. In HHPSO, the largest distance between the 'worst' particle \mathbf{x}_w and the global best \mathbf{g}_{best} will be considered as the length \mathcal{L} of achieved space. Then, we can trisect the length to classify the particles by two constants, but it may lead heavily imbalance at the late stage of search process due to the particles will trend to shrink the achieved space along with the search proceeding. Therefore, we introduce a nonlinear attenuation factor ϖ varying with time to condense the achieved space, and ϖ is defined as follows,

$$\varpi_{t+1} = \varpi_t \left(\frac{N_G \times k}{N_G^2 - k} \right)^{1/N_G} \quad (9)$$

where N_G and k are the maximum number of generations and current generation, respectively, and $\varpi_0 = 1.0$. As shown in Eq. (9), ϖ

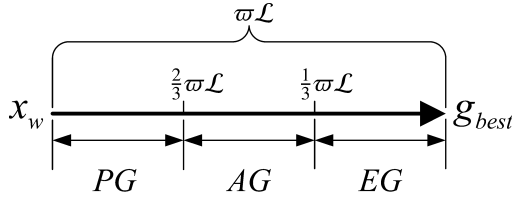


Fig. 4. Definition of the hierarchical groups: excellent group (EG), affiliated group (AG) and potential group (PG).

can efficiently trisect the achieve space when it decreases faster in initial stage than that in late stage of search process. ϖ will keep stable decrease as it approaching to the late stage. Depending on ϖ , we define the three groups as shown in Fig. 4. For instance, if the distance d between a particle and the global best g_{best} satisfies $d \leq 1/3\varpi\mathcal{L}$, this particle will be classified to group EG. If it is in $1/3\varpi\mathcal{L} < d \leq 2/3\varpi\mathcal{L}$, the particle will be grouped into AG, otherwise the particle will be set as a member of PG.

To coordinate closely with the potential group, a probability-based swarm migration is developed for avoiding inefficient search and neglecting most of the local minimums in the optimized landscape. Accordingly, the new hierarchical structure will be established and the details will be extended in following sections (Sections 3.2 and 3.3).

3.2. Information sharing mechanisms

If the particles converge at a high speed, they always tend to shrink towards local regions within a few generations [30–32]. The phenomenon leads to similar search behaviors among the particles and the loss of diversity in the swarm. If the particles fall into the local regions, they are unable to escape due to their homogeneous search behavior and lack of exploration ability. To improve the performance of PSO, the particles should be allowed to leave their original trajectories to explore the potential search space. Therefore, the heterogeneous search behaviors are designed in HHPSO, and, according to the hierarchical structure, the excellent particles (EPs) in EG, the potential particles (PPs) in PG and the affiliated particles (APs) in AG play different roles to achieve various tasks in the search process. The APs link the EPs and the PPs for the heterogeneous search. The EPs move around the global optimum in current search space, while the PPs will explore new areas for potential solutions. These designs not only maintains local search but also can seek out the global optimum based on knowledge from multiple local optima. Fig. 5 illustrates the search behaviors and the information exchange flow.

The positions of the particles are updated by Eqs. (10) and (12). The locations of EP, PP and AP at time t (black dots) and $t+1$ (color dots) are shown in Fig. 5. From the figure, at time t the positions of the particles are set randomly (the black dots), and the associated velocities are also set randomly as a black line. The statuses of the particles at time $t+1$ are updated according to the position Eq. (8) and the modifications of velocities in Eqs. (10) and (12). The new

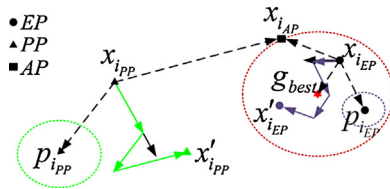


Fig. 5. Information exchange among the three groups. The filled circles, triangles and squares are the positions of the particles. The arrows stand for the potential flight directions.

search vectors for the unknown search space can be obtained from the equations. As shown in Eq. (10), the velocity of the particle \mathbf{x}_{iEP} employs the information of the AP to enhance the deep exploitation in small regions. The EPs can carry out a fine detailed search around the captured global optimum. Eq. (10) is used to refresh the velocity of the particle \mathbf{x}_{iEP} .

$$\begin{aligned} \mathbf{v}_{iEP}^j(k+1) = & \omega \cdot \mathbf{v}_{iEP}^j(k) + c_0 \cdot \mathbf{rand} \cdot (\mathbf{p}_{iAP}^j - \mathbf{x}_{iEP}^j(k)) \\ & + c_1 \cdot \mathbf{rand} \cdot (\mathbf{p}_{iEP}^j(k) - \mathbf{x}_{iEP}^j(k)) \\ & + c_2 \cdot \mathbf{rand} \cdot (\mathbf{g}_{best}^j - \mathbf{x}_{iEP}^j(k)) \end{aligned} \quad (10)$$

where **rand** is a vector consisting of random numbers, which subject to uniform random distribution function in the interval [0,1].

As a linkage, the APs should use the information from the EPs and the PPs to enhance their abilities. Accordingly, the update law of the APs is defined as follows,

$$\begin{aligned} \mathbf{v}_{iAP}^j(k+1) = & \omega \cdot \mathbf{v}_{iAP}^j(k) + c_1 \cdot \mathbf{rand} \cdot (\arg \max f(\mathbf{x}_{iEP}^j) - \mathbf{x}_{iAP}^j(k)) \\ & + c_2 \cdot \mathbf{rand} \cdot (\arg \min f(\mathbf{x}_{iPP}^j(k)) - \mathbf{x}_{iAP}^j(k)) \end{aligned} \quad (11)$$

As shown in Eq. (11), the velocity of each particle of AG is affiliated to the other two groups – EG and PG. For efficient search, we use the AP as the ‘virtual center’ of the PPs for exploring the potential zones. Therefore, the \mathbf{x}_{iPP} can be prevented from moving far away from the current center or out of the search space. The velocity of \mathbf{x}_{iPP} is updated using Eq. (12):

$$\begin{aligned} \mathbf{v}_{iPP}^j(k+1) = & \omega \cdot \mathbf{v}_{iPP}^j(k) + c_1 \cdot \mathbf{rand} \cdot (\mathbf{p}_{iPP}^j(k) - \mathbf{x}_{iPP}^j(k)) \\ & + c_2 \cdot \mathbf{rand} \cdot (\arg \max f(\mathbf{x}_{iAP}^j(k)) - \mathbf{x}_{iPP}^j(k)) \end{aligned} \quad (12)$$

According to Eq. (12), \mathbf{x}_{iPP} uses the position of an AP to refresh itself without directly using the position of the current global best particle. The PPs are attracted by the APs and able to conquer unknown space for potential solutions. It can be concluded from Eqs. (11) and (12), the role of the AP is the linkage of the EP and the PP for enhancing information exchange, so that they can cooperate with each other indirectly.

3.3. Probability-based swarm migration

In PSO, premature convergence is still a main problem. The particles, learning from the ‘global best’ even if it is only a local optimum, will be trapped in local region when PSO is used to deal with complex optimization with a highly rugged landscape [12]. Accordingly, probability-based swarm migration is developed to cross the regional barriers and avoids inefficient search. The particles in HHPSO are determined to move or not according to the value of the probability. The larger the value is, the more chance the particle has to migrate.

As a parameter of swarm migration, the migration probability plays an important role in HHPSO. In the whole swarm, each particle is assigned an executing migration probability p_{emi} to determine which particle is activated to move to the new center. Initially, equal probabilities are assigned for all particles, that is $p_{emi} = 1/n$, (n is the number of the particle).

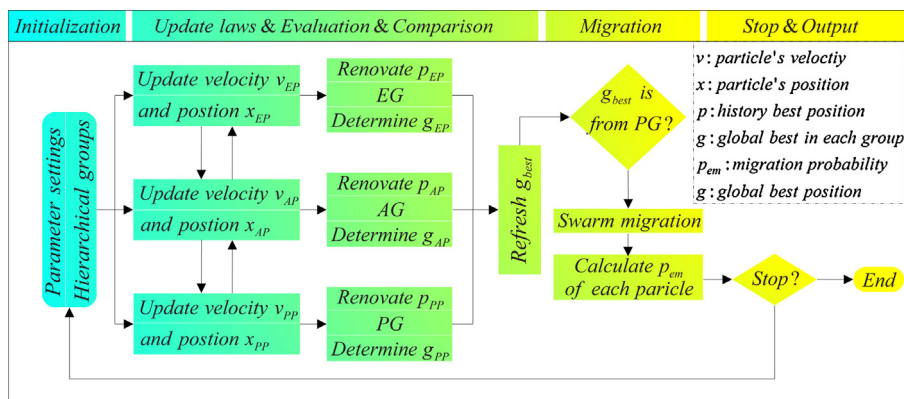


Fig. 6. System excogitation of the proposed algorithm – HHPSO. Three hierarchical groups (EG, AG, and PG) are designed to accomplish different search tasks in the defined solution space, and the PG plays a vital role in activating the swarm migration mechanism.

In order to define the formula used to calculate the probability p_{em_i} , it is necessary to define the normalized distance d_i and the fitness distance f_i as follows:

$$d_i = \exp \left(\frac{\| \mathbf{x}_{iEP} - \mathbf{g}_{best}^o \|}{\sum_{i=1}^{n_0} \| \mathbf{x}_{iEP} - \mathbf{g}_{best}^o \|} - 1 \right) \quad (13)$$

$$f_i = \exp \left(- \frac{(f_{\mathbf{x}_{iEP}} - f_{\mathbf{g}_{best}^c})^2}{2\theta^2 + mse^2} \right) \quad (14)$$

$$mse = \sqrt{\frac{\sum_{i=1}^{n_0} \| \mathbf{x}_{iEP} - \mathbf{g}_{best}^o \|^2}{n_0}} \quad (15)$$

where \mathbf{g}_{best}^o is the original center. The $f_{\mathbf{x}_{iEP}}$ and $f_{\mathbf{g}_{best}^o}$ stand for the i th particle fitness value and the achieved best value, respectively. θ denotes as a regulator of fitness distance, which increases or decreases the length of decay of the exponential. Then the migration probability p_{em_i} is obtained as follows:

$$p_{em_i}(k) = \frac{f_i d_i \sqrt{MSE}}{\sum_{i=1}^{n_0} f_i d_i \sqrt{MSE}} \quad (16)$$

where n_0 is the size of the EPs in the original swarm. According to Eq. (16), EPs with larger values of $f_i d_i \sqrt{MSE}$ are more likely to get activated and migrate.

$$MSE = \sqrt{\frac{\sum_{i=1}^{n_0} (\mathbf{x}_{iEP} - \mathbf{g}_{best}^c)^2}{n_0}} \quad (17)$$

where \mathbf{g}_{best}^c is the center of the target swarm.

The above migration probability is utilized to conduct the swarm migration for the two reasons as follows:

- By taking the EPs fitness values into account in the probability p_{em_i} , an EP, whose fitness value is close to the best in the original swarm, should be activated to migrate first, because it is no longer necessary to explore around this local optimum.
- By taking the distance into account in the probability p_{em_i} , any two EPs that have small spatial distance are also close to each other in the original swarm. To keep the diversity of potential solutions and the migration stable, EPs in a crowded cluster have higher probability to move to the newly constructed center.

Migration is activated gradually to prevent the swarm moving too quickly, which may result in another local optimum. The activated EPs follow migration strategy for updating as shown in Eq. (18).

$$\mathbf{x}_{EP} = (\mathbf{g}_{best}^c - \mathbf{g}_{best}^o) + (2 \cdot \text{rand} - 1) \cdot \mathbf{R} \quad (18)$$

where $\mathbf{R} = \| \mathbf{g}_{best}^o - \arg \max f(\mathbf{x}_{iAP}) \|$ stands for the maximum distance between the original global best \mathbf{g}_{best}^o and an affiliated particle. \mathbf{g}_{best}^c is the newly optimal achievement.

In the swarm migration, the original global position is no longer the best one, but it can be set as a local optimum for developing the exploration information. Meanwhile, it can have an effect on tracking the past directions. During the migration, the information about the achieved global optimum is shared between the initial swarm and the emerging one. The information can also be obtained by the EPs in the new area. When the swarm migration completes, it is necessary to achieve new hierarchical EG, PG and AG.

The system excogitation of the HHPSO algorithm is illustrated in Fig. 6.

4. Simulation experiments and discussion

In this section, we present HHPSO to minimize the potential energy function of a scalable molecule with different dimensions (from 20 to 200) and a realistic energy function of pseudo-ethane molecule. The performance of HHPSO is compared with six PSO variants and four GA-based methods over these two minimization problems. Experiments over the problems are performed on 64-bit operating system with intel (R) Core (TM) i7-3770 CPU (3.40 GHz) and 8G of RAM. This section involves parameter effects in HHPSO, parameter settings of all PSO variants, experimental results, discussion and their statistic analysis.

4.1. Effect of parameters

HHPSO has a number of control parameters, which may have significant effects on its performance. In this section, we discuss the influence of three main parameters used in the HHPSO algorithm. These three parameters consist of the fitness similarity regulator θ , and the learn factors. Experiments are conducted on functions F_1 – F_6 [33] with 30 dimensions to investigate the impact of these three parameters. The design of experiments (DOE) were conducted for all three the parameters, and in DOE the learn factors were separated into two groups, that is, c_0 and $c_1 = c_2$. The maximum number of generations N_G was set to $N_G = 1000$. The inertia weight ω is set to $\omega = 0.9 - 0.5k/N_G$. The other setups of HHPSO are presented in Section 4.2. The mean errors between the best-so-far values and the desired optimal values are used to measure the performance of HHPSO.

Fig. 7 illustrates the investigation of the effect of the three parameters concluding from the main effect of DOE, and the results were normalized over each benchmark function. In the HHPSO algorithm, θ is used to control the distance among the particles

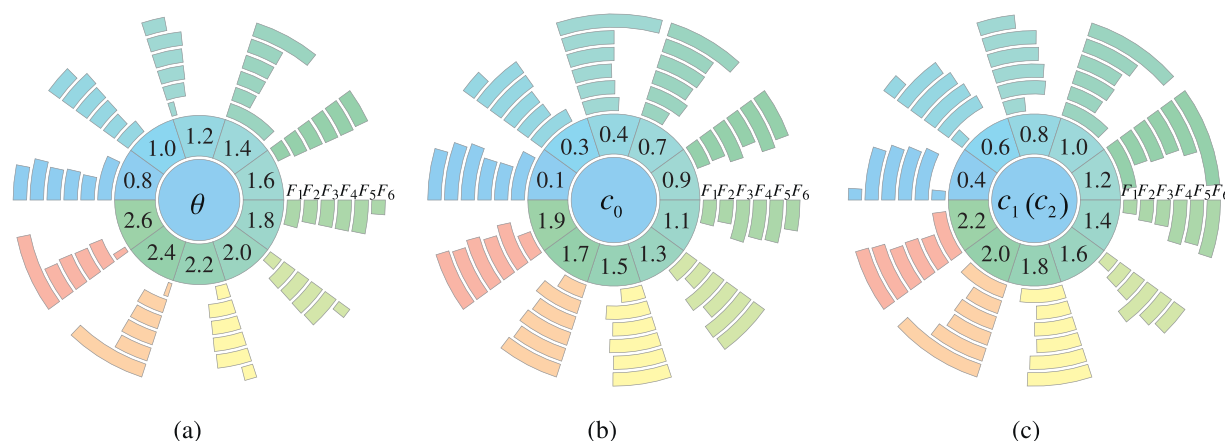


Fig. 7. The main effect of the three control parameters in HHPSO concluded from DOE: (a) the main effect of the fitness similarity regulator θ , (b) the main effect of learning factor c_0 , and (c) the main effect of learning factor $c_1 = c_2$.

according to the fitness values. With the help of θ , the operation of the swarm migration can be easily implemented to adjust the migration in HHPSO. The main effects over the six benchmark functions with different values are exhibited in Fig. 7(a). In the proposed algorithm, we employ an additional learning factor c_0 , and it is necessary to analyze the effect of these learning factors, which may lead to various performance of HHPSO. In DOE, we vary the value of c_0 from 0.1 to 1.9 in increments of 0.2, and its main effect is illustrated in Fig. 7(b). The values of c_1 and c_2 are equal and vary from 0.4 to 2.2 in increments of 0.2. Fig. 7(b) illustrates the main effect of $c_1 = c_2$ on HHPSO. According to the average results over the six benchmark functions in DOE, the three parameters in HHPSO are set to $\theta = 1.0$, $c_0 = 1.1$, and $c_1 = c_2 = 1.49445$, respectively.

4.2. Parameters settings

In this section, the compared PSO variants are listed in Table 1, in which the parameters are fixed in all the experiments of this study. These PSO variants include SPSO [34], FDRPSO [11], UPSO [35], CLPSO [30], APSO [36], and CHPSO [14], and the parameters of each PSO variant are shown in Table 1.

Different parameter values can have different effects on algorithm performance. Hence, the parameters in Table 1 are selected based on the suggestions in the original references. Besides the parameters listed in Table 1, other ones are also recommended in the related references. In this study, the maximum number of fitness evaluations are set to $N_G \times 40$ (N_G is set to 2000) and 4×10^6 for the potential energy functions of a scalable molecule and a pseudo-ethane molecule, respectively.

4.3. Experiments over simplified molecular potential energy function

The proposed HHPSO was compared to SPSO [34], FDRPSO [11], UPSO [35], CLPSO [30], APSO [36], and CHPSO [14]. The experiments

Table 2

Global minimum value G_m for chains of different sizes D .

D	G_m	D	G_m
20	−0.82237	90	−3.70065
30	−1.23355	100	−4.11183
40	−1.64473	120	−4.93420
50	−2.05592	140	−5.75656
60	−2.46710	160	−6.57893
70	−2.87828	180	−7.40129
80	−3.28946	200	−8.22366

were conducted for the problem on searching the 3D structure with the minimal energy of a molecule by varying the dimension from 20 to 90 increasing by 10 and from 100 to 200 in increments of 20, each of which run 50 independently. All the results were recorded to compare and analyze the performances of the PSO variants. Table 2 shows that the global minimum values vary with the scale of the problem. In Table 3, the experimental results of all the compared PSO variants are summarized and the best ones are in bold.

Table 3 shows the dimension and the associating global minimum of the energy function, and the results of the compared PSO variants are also presented. As shown, it becomes hard for all the PSO variants to achieve the global solution as the dimension increasing. Although SPSO is the worst one over the energy function with dimension $D \leq 120$, it is better than CLPSO from $D = 140$ to 200 in increments of 20. Over all dimensions, however, the standard deviation (std.) results achieved by SPSO is the largest. The average (avg.) results of FDRPSO, UPSO, APSO, and CHPSO were similar to each other, but in detailed the std. of CHPSO is much larger when the dimension is set to 140, while those of the other three methods (FDRPSO, UPSO, and APSO) are increasing with the dimensions becoming larger.

The proposed HHPSO achieved the results with smaller avg. and std. as illustrated in Fig. 8. It is interesting to find that the

Table 1

The parameters of the PSO variants.

Algorithm	Parameters		
	Population size	Inertia weight	Acceleration coefficient
SPSO [34]	$n = 40$	$\omega(k) = 1/(2\log(2))$	$c_1 = c_2 = 0.5 + \log(2)$
FDRPSO [11]	$n = 40$	$\omega(k) = 0.9 - 0.5k/N_G$	$c_1 = c_2 = 1.0$, $c_3 = 2.0$
UPSO [35]	$n = 40$	$\omega(k) = 0.729$	$c_1 = c_2 = 1.49445$
CLPSO [30]	$n = 40$	$\omega(k) = 0.9 - 0.7k/N_G$	$c_1 = c_2 = 1.49445$
APSO [36]	$n = 40$	$\omega(k)^* = 0.9$	$c_1 = c_2 = 2.0$
CHPSO [14]	$n = 4 \times 10$	$\omega(k) = 0.9 - 0.5k/N_G$	$c_1 = c_2 = 1.49445$
HHPSO	$n = 40$	$\omega(k) = 0.9 - 0.5k/N_G$	$c_0 = 1.1$, $c_1 = c_2 = 1.49445$

s^* represents the initial inertia weight.

Table 3
The results of all the compared PSO variants over the problem of searching the 3D structure.

D	Algorithm						
	SPSO	FDRPSO	UPSO	CLPSO	APSO	CHPSO	HHPSO
20	1.115 ± 1.508	−0.022 ± 0.202	0.012 ± 0.211	−0.822 ± 0.000	−0.102 ± 0.162	−0.030 ± 0.142	−0.822 ± 0.000
30	2.568 ± 3.702	0.047 ± 0.289	−0.028 ± 0.233	−1.232 ± 0.012	−0.066 ± 0.256	0.076 ± 0.335	−1.234 ± 0.000
40	2.616 ± 3.847	0.209 ± 0.326	0.035 ± 0.304	−1.639 ± 0.012	−0.154 ± 0.246	0.368 ± 1.115	−1.645 ± 0.000
50	2.143 ± 2.830	0.127 ± 0.388	0.115 ± 0.375	−1.975 ± 0.037	−0.111 ± 0.267	0.125 ± 0.664	−2.056 ± 0.000
60	3.245 ± 5.087	0.063 ± 0.379	0.140 ± 0.365	−1.962 ± 0.155	−0.145 ± 0.325	0.330 ± 1.659	−2.467 ± 0.000
70	3.396 ± 5.200	0.154 ± 0.408	0.098 ± 0.488	−1.613 ± 0.235	−0.088 ± 0.332	0.173 ± 0.745	−2.878 ± 0.000
80	3.154 ± 5.765	0.163 ± 0.406	0.210 ± 0.399	−1.002 ± 0.288	−0.247 ± 0.318	0.045 ± 0.473	−3.290 ± 0.000
90	3.494 ± 5.085	0.292 ± 0.514	0.298 ± 0.562	−0.267 ± 0.378	−0.270 ± 0.313	0.076 ± 1.033	−3.701 ± 0.000
100	4.215 ± 7.552	0.225 ± 0.527	0.374 ± 0.585	0.621 ± 0.430	−0.336 ± 0.418	0.140 ± 0.681	−4.112 ± 0.000
120	6.064 ± 11.300	0.275 ± 0.667	0.359 ± 0.614	3.011 ± 0.566	−0.262 ± 0.363	−0.017 ± 0.163	−4.933 ± 0.002
140	4.753 ± 6.205	0.576 ± 0.668	0.380 ± 0.570	6.134 ± 0.934	−0.207 ± 0.478	0.326 ± 2.524	−5.459 ± 0.164
160	5.027 ± 2.989	0.569 ± 0.996	0.783 ± 1.050	10.143 ± 1.033	−0.026 ± 0.677	0.269 ± 1.193	−4.276 ± 0.375
180	7.155 ± 9.167	1.652 ± 1.249	1.100 ± 1.033	15.352 ± 1.204	0.104 ± 0.652	0.149 ± 0.902	−3.004 ± 0.465
200	7.752 ± 8.558	2.234 ± 1.429	2.232 ± 1.114	20.811 ± 1.544	0.593 ± 1.018	0.120 ± 0.784	−1.179 ± 0.779

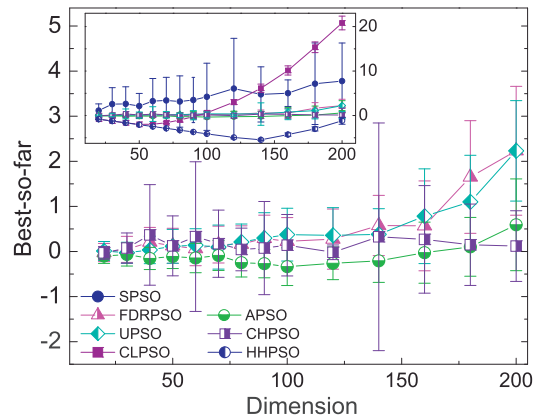


Fig. 8. The experimental results of all compared PSO variants over the potential energy function with different dimensions.

performances of HHPSO exhibits two different characteristics separated by $D = 140$. HHPSO can figure out a solution approaching to the global minimum as the dimension increasing when it is used to solve the problem of minimizing the potential energy with $D \leq 140$, that is, HHPSO can efficiently achieve the most stable conformation of a molecule with chain size less than or equal to 140. On the other hand, HHPSO still can achieve better results than the compared PSO variant although its best-so-far results become worse over the problem with $D > 140$ comparing with itself on $D \leq 140$.

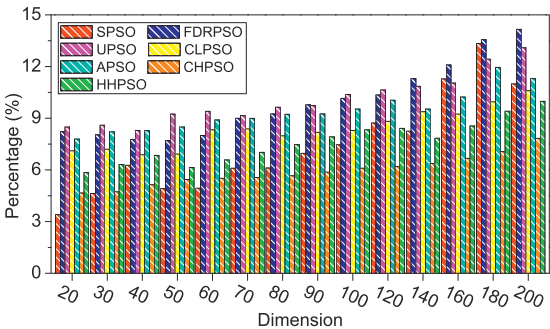


Fig. 9. The results of all compared PSO variants over the energy function with different dimensions.

In the experiments of finding the minimum potential energy, the computational efficiency P_{CE} of each PSO variants is used to compare their performances according to CPU time. The percentage P_{CE} is defined depending on the run time of each algorithm and the total computational time of all the algorithms over the problem of searching the most stable structure of a molecule with a fixed scale (dimension D), and it is formulated as shown in Eq. (19).

$$P_{CE} = \frac{T_e(D)}{T_{tot}(D)} \times 100\% \tag{19}$$

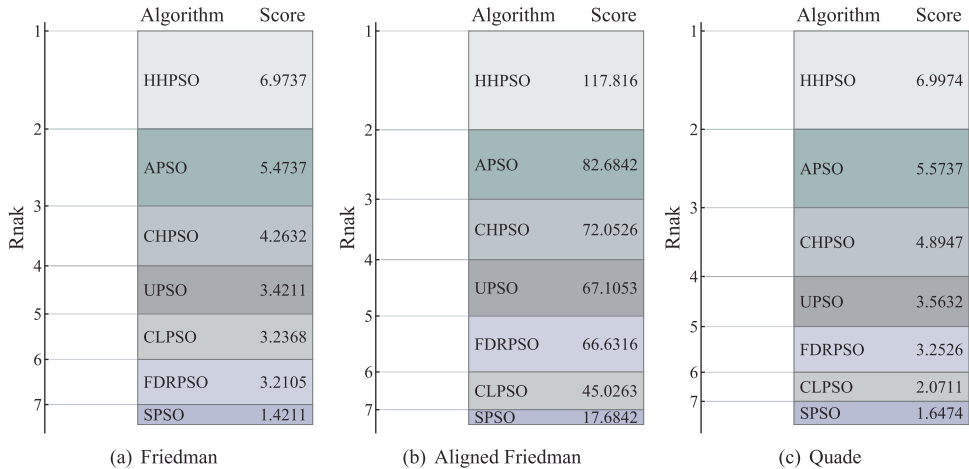


Fig. 10. Average ranks and scores of all PSO variants over molecular potential energy function with different dimensions: (a) Friedman (statistic: 78.479323, p -value: 0); (b) Aligned Friedman (statistic: 16.190596, p -value: 0.012766711047); (c) Quade (statistic: 28.357476, p -value: 0).

Table 4

Experimental results over the pseudo-ethane molecule.

Algorithm	FES_{avg}	FES_{std}	FES_{min}	FES_{max}	SR	Time (s)
GA	2,169,771	1,097,602	274,424	3,251,614	15/30	2498
HYB	2,250,450	849,153	692,753	3,173,252	11/30	2653
rHYB	2,078,647	1,092,403	791,081	3,245,070	7/30	2855
oHYB	394,534	109,650	157,400	671,526	19/30	1131
PSO	284,316	203,789	149,342	581,295	18/30	1082
FDRPSO	258,952	125,861	254,137	437,519	21/30	1034
FRPSO	21,345	8262	10,641	38,233	29/30	845
HHP SO	20,880	5248	10,248	32,025	30/30	505

where T_e stands for the computational time of an algorithm on the fixed dimension D , while T_{tot} is the total time of all the algorithms on the D -dimensional problem.

The computational efficiency of each PSO variant is illustrated in Fig. 9. As shown in the figure, CHPSO is the best one on average computational time. FDRPSO and UPSO are the top two time-consuming methods among all the seven PSO variants, while CLPSO and APSO are a little better than the FSRPSO and USPO. In most cases, the computational time of SPSO is increasing with the dimension of the optimization problem as well as the HHP SO.

To compare the seven algorithms further, the Friedman, Aligned Friedman, and Quade tests [37] are used to analyze the performance of all algorithms. The statistical analysis for ranking the performance are conducted on the problem of minimizing the potential energy function of a molecule, and the average rankings are listed in Fig. 10. The higher the score is, the better the performance is. Each algorithm and its score are listed in descending order. The statistics and the corresponding p -values are shown in figure caption (Fig. 10). As shown, the proposed HHP SO earns the best score on each of the non-parametric statistical analysis. In terms of the computed p -values, there exists significant differences among the algorithms with $\alpha = 0.05$.

4.4. Experiments over potential energy function of pseudo-ethane

This section presents the experiments on minimizing the potential energy of pseudo-ethane. The experiment is to find the most stable conformation, whose global minimum energy value is 1.0711, of the pseudo-ethane molecule [1]. The number of independent trials and the maximum number of fitness evaluations (FEs) are set to 30 and 4×10^6 . The criterion of stopping evaluation is that the best-so-far result is equal to or better than a threshold of 99% of the global minimum. All the results of each trail are recorded (the best results are in bold) and compared with other seven methods, involving four GA-based method [23] and three PSO-based methods [4], in Table 4.

As shown in Table 4, FES_{avg} , FES_{std} , FES_{min} and FES_{max} are the average, standard deviation, minimum and maximum values of fitness evaluations, respectively. SR is the number of successful trails, which achieve the threshold, among all independent ones. Among all the comparing algorithms, HHP SO achieves the best results in term of FES_{avg} and FES_{std} but consumes less CPU time in the search process.

5. Conclusions

The paper presents a hierarchical particle swarm optimizer for minimizing the potential energy of molecular structure. In the proposed algorithm, the population is classified into three hierarchical groups (EG, PG, and AG), which are determined by a nonlinear variable combining with the distance between the particle and the achieved global optimum. The AG is not only affiliated to the EG and the PG but also links them, therefore, they can effectively cooperate with others and update themselves according to their own update

laws. The PG is promised to explore unknown areas, while the EG is assigned to accomplish the search in the region around the achieved global minimum. As an affiliated group, the AG attracts the PG to avoid losing its search direction, and it also guarantees that the EG can share the differences between AG and PG directly or indirectly without trapping into local regions. Coordinating with the PG, a probability-based swarm migration is to prevent unpromising search and wasting too much time in improper regions. Based on results on the problems of minimizing the potential energy, it can be concluded that HHP SO significantly improves PSO's search ability and exhibits better results when compared to other six PSO variants with p -value < 0.0128 .

Acknowledgments

This work was supported by China Scholarship Council, the National Natural Science Foundation of China (61222306, 91130033, 61175024), Shanghai Science and Technology Commission (11JC1404800), a Foundation for the Author of National Excellent Doctoral Dissertation of PR China (201048), and Program for New Century Excellent Talents in University (NCET-11-0330).

References

- [1] C.D. Maranas, C.A. Floudas, Global minimum potential energy conformations of small molecules, *J. Glob. Optim.* 4 (2) (1994) 135–170.
- [2] M. Dražić, C. Lavor, N. Maculan, N. Mladenović, A continuous variable neighborhood search heuristic for finding the three-dimensional structure of a molecule, *Eur. J. Oper. Res.* 185 (3) (2008) 1265–1273.
- [3] J.C. Bansal, K. Shashi Deep, V.K. Katiyar, Minimization of molecular potential energy function using particle swarm optimization, *Int. J. Appl. Math. Mech.* 6 (9) (2010) 1–9.
- [4] S. Agrawal, S. Silakari, Fletcher–Reeves based particle swarm optimization for prediction of molecular structure, *J. Mol. Graph. Model.* 49 (2014) 11–17.
- [5] J. Kennedy, R.C. Eberhart, Particle swarm optimization, in: *Proceedings of the IEEE Conference, IEEE Service Center, Perth, Australia, 1995*, pp. 1942–1948.
- [6] Y. Shi, R.C. Eberhart, A modified particle swarm optimizer, in: *Proceedings of the Conference on Evolutionary Computation, IEEE Press, Piscataway, 1998*, pp. 69–73.
- [7] M. Clerc, J. Kennedy, The particle swarm-explosion, stability, and convergence in a multidimensional complex space, *IEEE Trans. Evol. Comput.* 6 (1) (2002) 58–73.
- [8] A. Ratnaweera, S. Halgamuge, H. Watson, Self-organizing hierarchical particle swarm optimizer with time-varying acceleration coefficients, *IEEE Trans. Evol. Comput.* 8 (3) (2004) 240–255.
- [9] A. Chatterjee, P. Siarry, Nonlinear inertia weight variation for dynamic adaptation in particle swarm optimization, *Comput. Oper. Res.* 33 (2006) 859–871.
- [10] P. Suganthan, Particle swarm optimiser with neighbourhood operator, in: *Proceedings of the 1999 Congress on Evolutionary Computation*, vol. 3, 1999, pp. 1958–1962.
- [11] T. Peram, K. Veeramachaneni, C.K. Mohan, Fitness-distance-ratio based particle swarm optimization, in: *Proceeding in Swarm Intelligence Symposium, 2003*, pp. 174–181.
- [12] F.V. den Bergh, A.P. Engelbrecht, A cooperative approach to particle swarm optimization, *IEEE Trans. Evol. Comput.* 8 (3) (2004) 225–239.
- [13] M. Montes de Oca, J. Pena, T. Stutzle, C. Pinciroli, M. Dorigo, Heterogeneous particle swarm optimizers, in: *IEEE Congress on Evolutionary Computation, 2009*, pp. 698–705.
- [14] N.J. Cheung, X.-M. Ding, H.-B. Shen, OptiFel: a convergent heterogeneous particle swarm optimization algorithm for Takagi–Sugeno fuzzy modeling, *IEEE Trans. Fuzzy Syst.* 22 (4) (2014) 919–933, <http://dx.doi.org/10.1109/TFUZZ.2013.2278972>.

- [15] B. Leonard, A. Engelbrecht, A. van Wyk, Heterogeneous particle swarms in dynamic environments, in: IEEE Symposium on Swarm Intelligence, 2011, pp. 1–8.
- [16] S. Janson, M. Middendorf, A hierarchical particle swarm optimizer and its adaptive variant, *IEEE Trans. Syst. Man Cybern. B: Cybern.* 35 (6) (2005) 1272–1282.
- [17] Y. Peng, B.-L. Lu, A hierarchical particle swarm optimizer with Latin sampling based memetic algorithm for numerical optimization, *Appl. Soft Comput.* 13 (5) (2013) 2823–2836.
- [18] S. Alam, G. Dobbie, Y. Koh, P. Riddle, Clustering heterogeneous web usage data using hierarchical particle swarm optimization, in: 2013 IEEE Symposium on Swarm Intelligence (SIS), 2013, pp. 147–154.
- [19] C.-F. Juang, C.-M. Hsiao, C.-H. Hsu, Hierarchical cluster-based multispecies particle-swarm optimization for fuzzy-system optimization, *IEEE Trans. Fuzzy Syst.* 18 (1) (2010) 14–26.
- [20] P. Ghosh, H. Zafar, S. Das, A. Abraham, Hierarchical dynamic neighborhood based particle swarm optimization for global optimization, 2011 IEEE Congress on Evolutionary Computation (CEC) (2011) 757–764.
- [21] R.A. Engh, R. Huber, Accurate bond and angle parameters for X-ray protein structure refinement, *Acta Crystallogr. A* 47 (4) (1991) 392–400.
- [22] C. Lator, N. Maculan, A function to test methods applied to global minimization of potential energy of molecules, *Numer. Algorithms* 35 (2–4) (2004) 287–300.
- [23] H.C. Barbosa, C.C. Lator, F.M. Raupp, A GA-simplex hybrid algorithm for global minimization of molecular potential energy functions, *Ann. Oper. Res.* 138 (1) (2005) 189–202.
- [24] J.T. MacDonald, L.A. Kelley, P.S. Freemont, Validating a coarse-grained potential energy function through protein loop modelling, *PLoS ONE* 8 (6) (2013) e65770.
- [25] J.L. Klepeis, M.J. Pieja, C.A. Floudas, Hybrid global optimization algorithms for protein structure prediction: alternating hybrids, *Biophys. J.* 84 (2) (2003) 869–882.
- [26] B.-I. Koh, A.D. George, R.T. Haftka, B.J. Fregly, Parallel asynchronous particle swarm optimization, *Int. J. Numer. Methods Eng.* 67 (4) (2006) 578–595.
- [27] J.F. Schutte, R.T. Haftka, B.J. Fregly, Improved global convergence probability using multiple independent optimizations, *Int. J. Numer. Methods Eng.* 71 (6) (2007) 678–702.
- [28] J.J. Durillo, A.J. Nebro, F. Luna, C.A. Coello Coello, E. Alba, Convergence speed in multi-objective metaheuristics: efficiency criteria and empirical study, *Int. J. Numer. Methods Eng.* 84 (11) (2010) 1344–1375.
- [29] R.S. Parpinelli, F.R. Teodoro, H.S. Lopes, A comparison of swarm intelligence algorithms for structural engineering optimization, *Int. J. Numer. Methods Eng.* 91 (6) (2012) 666–684.
- [30] J.J. Liang, A.K. Qin, P.N. Suganthan, S. Baskar, Comprehensive learning particle swarm optimizer for global optimization of multimodal functions, *IEEE Trans. Evol. Comput.* 10 (3) (2006) 281–295.
- [31] S.-T. Hsieh, T.-Y. Sun, C.-C. Liu, S.-J. Tsai, Efficient population utilization strategy for particle swarm optimizer, *IEEE Trans. Syst. Man Cybern. B: Cybern.* 39 (2) (2009) 444–456.
- [32] Y. Wang, B. Li, T. Weise, J. Wang, B. Yuan, Q. Tian, Self-adaptive learning based particle swarm optimization, *Inf. Sci.* 181 (20) (2011) 4515–4538.
- [33] P.N. Suganthan, N. Hansen, J.J. Liang, K. Deb, Y.P. Chen, A. Auger, S. Tiwari, Problem Definitions and Evaluation Criteria for the CEC 2005 Special Session on Real Parameter Optimization, Tech. Rep., Nanyang Technological University, 2005.
- [34] M. Omran, Standard Particle Swarm Optimisation, 2012 http://clerc.maurice.free.fr/pso/SPSO_descriptions.pdf
- [35] K.E. Parsopoulos, M.N. Vrahatis, UPSO: A Unified Particle Swarm Optimization Scheme Lecture Series on Computer and Computational Sciences, vol. 1, 2004, pp. 868–873.
- [36] Z.-H. Zhan, J. Zhang, Y. Li, H.-H. Chung, Adaptive particle swarm optimization, *IEEE Trans. Syst. Man Cybern. B: Cybern.* 39 (6) (2009) 1362–1381.
- [37] J. Derrac, S. García, D. Molina, F. Herrera, A practical tutorial on the use of nonparametric statistical tests as a methodology for comparing evolutionary and swarm intelligence algorithms, *Swarm Evol. Comput.* 1 (1) (2011) 3–18.